Experimental and analytical behaviour of sandwich composites with glass fiber-reinforced polymer facings and layered fiber mat cores

Lauren MacDonnell and Pedram Sadeghian[1]

Department of Civil and Resource Engineering, Dalhousie University, 1360 Barrington Street, Halifax, NS, B3H 4R2, Canada

ABSTRACT:

This paper presents the results of experimental and analytical studies on the behaviour of sandwich beams fabricated with layered cores and glass fiber-reinforced polymer (GFRP) composite facings. The GFRP facings were fabricated using a unidirectional fiberglass fabric and epoxy resin, and the cores were fabricated using a thin non-woven continuous-strand polyester fiber mat with a thickness of 4.1 mm. A total of 30 sandwich beams with the width of 50 mm were prepared tested with five varying core configurations including cores made with one, two, or three layers of the fiber mat core and with or without the inclusion of intermediate GFRP layers. The specimens were tested up to failure under four-point bending at two different spans to characterize flexural and shear properties of the specimens. Two types of failure were observed, namely crushing of the compression facesheet and core shear. The load-deflection, load-strain, and moment-curvature behaviour were analyzed and using the results the flexural stiffness, shear stiffness, and core shear modulus were calculated. An analytical model was also developed to predict load-deflection behaviour and failure loading of sandwich specimens with varying core layouts. After verification, the analytical model was used for a parametric study of cases not considered in the experimental study, including additional GFRP and fiber mat core layers. It

[1] Corresponding author: Assistant Professor and Canada Research Chair in Sustainable Infrastructure, Email: Pedram.Sadeghian@dal.ca

was shown that additional fiber mat core layers and the inclusion of intermediate GFRP layers can increase the strength and overall stiffness of a sandwich beam, while additional GFRP layers can only increase the overall stiffness of the system. The analytical model can be used to optimize the configuration of layered sandwich composites for cost effective rehabilitation techniques of culverts, pipelines, and other curved-shape structures where a thin, flexible core is needed to accommodate the curvature of the existing structure.

KEYWORDS: Sandwich composite; fiber mat core; layered structure; GFRP; test; model.

DOI: https://doi.org/10.1177/0021998320939625

1. INTRODUCTION

Structural sandwich systems are used in a variety of structures as a lightweight material that also maintains the strength and stiffness required for a given application. Sandwich composite are composed of two thin, high-strength fiber-reinforced polymer (FRP) composite facesheets bonded to a lower density and generally weaker core material [1]. These structures are lighter than traditional materials such as steel and can be used to improve the structural efficiency of the system. Sandwich structures have been used in aerospace and marine applications but are growing in popularity in civil engineering applications; being used for wall, floor, and roof paneling for housing construction and for bridge construction [2]. The FRPs used as facings for sandwich panels can vary, and there have been studies on the use of synthetic fibers such as glass [3][4][5] and natural fibers such as flax [6][7][8]. The high-strength facesheets serve to resist the tensile and compressive forces that create a bending moment, while the core acts to resist shear and to stabilize the facesheets against wrinkling [9].

A variety of core materials have been used in the fabrication of sandwich panels and beams to date. Stiffer cores include the use of aluminum honeycombs and balsa wood, while more flexible core materials include foam cores such as polyurethane, polyvinyl chloride (PVC), polyethylene terephthalate, and phenolic cores [10][11][12]. Flexible thin cores have the advantage of being used in non-conventional applications such as curved surfaces for the rehabilitation of culverts and pipes. For thin multilayer cores, additional FRP layers can be added between the core layers; these are referred to as intermediate layers. Intermediate layers have been shown to increase the overall stiffness, strength, and impact resistance of a composite sandwich structure [13][14]. The use of FRP intermediate layers allows for the construction of curved shapes, as thin cores are more flexible than thick cores to shape a curve. As the core and facing of the sandwich structure can be cured at the same time, this can improve the connection between the two layers and minimize the risk of delamination or debonding. However, a major challenge of using conventional cores (e.g. foam, honeycomb, etc.) for curve-shaped composites is manufacturing and slicing the core into thin sheets to be applied for small radius carves. As the radius of a curve become smaller, a thinner sheet of core is needed. A thin layer of core is very fragile to be handled and applied for sandwich composites, especially in construction sites. The use of thin, three-dimensional (3D) woven fabric cores is another option, however previous study [15] showed that the 3D core was not stiff enough in shear to provided expected composite action between the facesheets.

There is another form of core material available in the market known as fiber mat, core mat, or bulker mat (hereafter called fiber mat). Fiber mats are fabricated by mixing micro-balloons into a matrix made of metal or polymer [16][17]. Fiber mats are usually used like another layer of fabric to be impregnated with the laminating resin during composite

construction. They come in the form of a flexible rolled sheet made of non-woven synthetic fibers (typically polyester fibers) and hollow micro-balloons, typically about 50% by volume of fiber mat. The micro-balloons displace resin and so the resultant layer has lower density than the equivalent thickness of solid laminates. However, cured impregnated fiber mats are denser than a conventional core. Fiber mats can easily accommodate two-dimensional curved-shape application with a small radius curvature.

The behaviour of sandwich composites with fiber mat cores were initially studied by Mines et al. [18] and Mines and Jones [19] in mid-ninety's. It was found that the fiber mat core used in the studies with thicknesses ranging from 8-11 mm were strong enough to lead the sandwich composites to the upper facesheet compressive failure. A decade later, Kolat et al. [20] studied the effect of the environmental degradation on the fracture toughness of sandwich composites made of different cores including a 13-mm thick fiber mat core. It was found that the fracture toughness of sandwich composites with fiber mat core was higher compared with its counterparts made of wood, plywood, and polyurethane core materials. Aquino et al. [21] used a 2-mm thick fiber mat with jute fabric facings and observed a good adherence between the jute fabric and the fiber mat core, however a premature shearing fracture of the fiber mat core was observed under both dry and wet conditions. Russo and Zuccarello [22] tested sandwich composites with a 4-mm thick fiber mat and found a significant shear non-linearity. It was also concluded that transverse stresses significantly influence the core shear failure of the sandwich beams with the fiber mat core. Recently, Ude et al. [23] studied the impact damage characteristics in reinforced woven natural silk/epoxy composite facesheet and 5-mm thick fiber mat. It was found that specimens with fiber mat core possessed better load bearing capability than other cores.

As it was highlighted in the literature, the behavior of sandwich composites with fiber mat core can be affected significantly with the shear behaviour and nonlinearity of the core material. In addition, there are some controversial understanding of the behaviour of the fiber mat cores. As fiber mat core materials are suggested [20] for structures with moderate strength requirements and where the thickness is important, the current study focusses on layering fiber mat cores and reinforcing the core with intermediate FRP layers to reach desirable strength and stiffness. In this study, layered sandwich beams were constructed using a 4.1-mm thick fiber mat core and glass FRP (GFRP) facings. Varying numbers of core layers and with or without the inclusion of intermediate GFRP layers were considered. The aim of the study is to evaluate and analyze the performance of the fiber mat core in the form of flat sandwich beams for future studies for curved-shape structures.

2. EXPERIMENTAL STUDY

2.1 Test Matrix

As shown in Table 1, a total of 30 sandwich composite beam specimens were fabricated out of GFRP facing and fiber mat core materials and tested under four-point bending. The specimens were fabricated with 1, 2, or 3 layers of a thin, flexible fiber mat core with a thickness of 4.1 mm/ply. One layer of GFRP was used per each facesheet. Specimens with 2 or 3 layers of core were fabricated with and without intermediate GFRP layer(s) between each core layer as shown in Figure 1. Two different spans were used for each sandwich configuration as shown in Table 1. Three identical specimens were fabricated and tested for each case. The specimens are identified using the specimen identification (ID) system of FX-SY or FX-G-SY where X indicates the number of core layers, G indicates the presence of intermediate GFRP layer between core layers,

and Y indicates the span length. Specimens were tested at spans of 300 mm and 400 mm, except for the specimen with one layer of core, which was tested at a span of 300 mm and 200 mm to be able to reach to a failure.

2.2. Material Properties

For each GFRP facing, a unidirectional fiberglass fabric was used, having a dry weight of 915 g/m^2. The fabric is made up of glass fibers that, when dry, have a reported density of 2.55 g/cm^3, a tensile strength of 3240 MPa, a tensile elastic modulus of 72.4 GPa, and an ultimate elongation of 4.5%, reported by the manufacturer (QuakeWrap, Tucson, AZ, USA). The resin used for the fabrication of the sandwich composites is a high strength, low viscosity structural epoxy made of a base resin and a hardener with a 2 to 1 volumetric mix ratio, respectively. The resin has a tensile strength of 49.3 MPa and a tensile elastic modulus of 2.0 GPa, reported by the same manufacturer. The GFRP composite made of the fiberglass fabric and resin has a tensile strength of 587 MPa, a tensile elastic modulus of 27.4 GPa, an ultimate elongation (rupture strain) of 2.3%, and a breaking force of 611 N/mm (ply thickness of 1.3 mm), all as reported by the same manufacturer. A fiber volume fraction of 0.33 for the GFRP composite was obtained by the authors based on the densities of 2.55 g/cm^3 and 1.13 g/cm^3 for the dry fiberglass and resin matrix, respectively.

The fiber mat core used is a lightweight non-woven continuous-strand mat made of polyester fiber, containing 45% micro-balloons by volume. The core has a dry bulk density of 0.045 g/cm^3 reported by manufacturer (Toyo Cloth Co Ltd, Osaka, Japan). The fiber mat core has a thickness of 4.1 mm ± 0.5 reported by the manufacturer, with limited change in thickness during the curing process. The fiber mat is flexible before the application of the resin and absorbs 55% by volume (2.80 kg/m^2 of one layer of fiber mat) to reach a bulk density of 0.6~0.8

g/cm^3 after curing per the manufacturer. The cured fiber mat has a tensile strength of 6.38 MPa, a tensile elastic modulus of 1.19 GPa, and an elongation of 0.51%, all in the longitudinal direction of the roll as reported by the manufacturer. The tensile strength and modulus of the cured fiber mat in the transverse direction of the roll was reported 78% and 84% of that of in the longitudinal direction, respectively. The cured fiber mat has also a shear strength of 3.55 MPa, however the shear modulus was not reported by the manufacturer.

2.3. Specimen Fabrication

Each group of specimens were prepared on a clean flat surface covered with non-stick wax paper and was fabricated using the wet hand lay-up method. Both the fiberglass fabric and the fiber mat core were cut using scissors to cover an area of 500 mm by 500 mm. This created a larger sandwich panel and allowed for the fabrication of multiple specimens at once. The longitudinal direction of the fiber mat roll was aligned with the fibers of the unidirectional fiberglass fabric to mimic real application of the system. The epoxy and the hardener were thoroughly mixed until uniform color is achieved as recommended by the resin manufacturer. Then the mixture was applied using brushes on each layer of fiberglass or fiber mat until they were adequately saturated.

Each fiber mat layer was saturated by applying 1/3 of the required resin (2800 g/m^2) to the down side of the mat and the remaining resin was applied to the top side based on the protocol recommended by the fiber mat manufacturer. Each layer of the fiberglass fabric was also saturated by applying the required resin (813 g/m^2) recommended by the resin manufacturer. Each layer was smoothed out using a spatula to remove any pockets of air. At the end, a wax paper was placed on the top layer and smoothed out using a metal roller. A lightweight wooden board (600 mm x 600 mm x 12.5 mm particle board, 6.25 kg/m^2) was placed on top of the wax

paper to ensure a flat and smooth finished surface. The board was kept over the 48-hour curing time of the resin.

The sandwich panel was left in the lab (air conditioned at 23±2 ºC and 30~50% relative humidity) to cure for 48 hours and then the wax paper was removed, and the panel was left at room temperature to cure completely. After at least 7 days, smaller specimens were cut from the panels as shown in Figure 2. Specimens were cut to a width of 50 mm and to the specified length of 350 mm, 450 mm, or 250 mm using a band saw. The longitudinal direction of the beam specimens was parallel to the fiber direction of the unidirectional fiberglass layers. The specimens were then marked with a permanent marker to indicate specimen ID and where the loading would be applied and where the supports would be located during testing.

2.4. Test Setup and Instrumentation

As shown in Figure 3, the specimens were tested under four-point bending with a support span (S) and a loading span (L), equal to 2/11 of the support span. This was in accordance with the standards for testing sandwich beams in bending based on ASTM D7249 [24] and ASTM D7250 [25]. The tensile and compressive strains at mid-span were measured using strain gauges mounted longitudinally on the top and bottom face of each specimen. Two linear potentiometers (LPs) were used to measure the midspan deflection of each specimen. The strain gauges were used to obtain strain of facesheets at any given load step up to the failure. They were also used to calculate the mid-span curvature for further moment-curvature analyses. The displacement gauges were used to obtain mid-span deflection of each specimen for load-deflection analyses. All tests were performed using a universal testing machine under a displacement-controlled rate of 2 mm/min. The specimens were loaded up to failure and load, displacement, and strain data were collected using a digital data acquisition system at a frequency of 10 Hz.

3. EXPERIMENTAL RESULTS AND DISCUSSION

The following section details the failure modes, load-deflection, load-strain, moment-curvature, and the flexural and shear stiffness of the sandwich specimens tested. The test results and failure modes are summarized in Table 2.

3.1. Failure Modes

Two primary modes of failure were observed during the testing of the GFRP and fiber mat sandwich specimens: i) top facesheet crushing (TFC) and ii) core shear (CS). Table 2 presents the failure mode of the test specimens. After a primary mode of failure which was corresponding to the peak load, top facesheet debonding/wrinkling (TFD) failure was also observed. Although, debonding and wrinkling were not the primary mode of failure and were always observed after top facesheet crushing or core shear failures. Images of the two primary modes of failure can be seen in Figure 4. Top facesheet crushing was observed at the peak load across all the varieties of the specimens. It was mainly initiated in the loading span (i.e. between the point loads) due to the maximum bending moment and induced longitudinal compression stress in the top facesheet. However, a few times the initiation was observed to be under one of the loading rollers. This could be due to the localized effects of the loading roller on the facesheet and/or the core. For majority of the test specimens, instability of the top facesheet in the form of debonding and wrinkling was also observed as a secondary failure mode after the primary failure at the peak load. Core shear was observed in F2-G and F3-G specimens with shorter span (i.e. 300 mm) and was observed after the top facesheet crushing in one of the F1 specimens with a span of 200 mm. Overall, the crushing of the top GFRP facesheet of the specimens with one, two, and there layers of the fiber mat core, without additional GFRP layer in between, indicated that the layered core

was strong enough in shear leading to the top facesheet crushing failure. Adding the GFRP layer between the fiber mat layers increased the load capacity of the specimens and changed the failure mode of shorter specimens to core shear failure due to higher load.

3.2. Load-Deflection Behaviour

Figure 5 displays load-deflection diagrams based on the mid-span deflection for all specimens tested with a span of 300 mm for comparison. All the specimens displayed linear behaviour up to the peak load. As there was no sign of non-linearity, it can be concluded that the fiber mat core is stiff and strong enough in shear accommodating the composite action between the facesheets. This needs to be confirmed in the analytical section by comparison of the flexural stiffness obtained based on full-composite action and that of based on the experimental measurements. The overall stiffness of each specimen was calculated using the slope of the load-deflection diagram. It is referred as overall stiffness, as the slope of the load-deflection diagram includes both flexural and shear stiffness of the specimen. The average and standard deviation of peak load and overall stiffness of each groups is presented in Table 2. It indicates that increasing the number of fiber mat core layers lead to an increase in the overall stiffness of the sandwich beams as well as to an increase in the peak load. The addition of intermediate GFRP layers to the multilayered fiber mat cores had the effect of increasing the overall stiffness and peak load. For example, by adding intermediate GFRP layers to F3-S400 configuration making F3-G-S400 specimens, the overall stiffness and peak load increased 40% and 10%, respectively. This indicates that the intermediate GFRP layers are more effective on overall stiffness than strength. Also, the overall stiffness and strength of a layered sandwich beam can be significantly increased through the addition of intermediate GFRP layers without considerable changes in the core thickness.

3.3. Load-Strain Behaviour

The longitudinal strains of each test were recorded using strain gauges mounted to the center of the top and bottom facesheets of each specimen. Load-strain diagrams of the 300 mm span specimens are shown in Figure 6. The load-strain curves also displayed linear behaviour up to the peak load. The symmetricity of the diagrams with respect to the vertical axis indicates that the absolute values of the tensile and compressive strains are close during each of the tests. It means the location of the neutral axis should be around the mid-height of each specimen.

3.4. Moment-Curvature Behaviour

The moment at the mid-span of each specimen was calculated for all load levels. The curvature at each load level was obtained based on the slope of the strain profile at mid-span with strains obtained from strain gauges. The curvature was calculated as the sum of the absolute values of top and bottom strains over the total height of the sandwich specimen. Moment-curvature diagrams for specimens spanning 300 mm are shown in Figure 7. All the specimens displayed linear moment-curvature behaviour during testing. The flexural stiffness D of each specimen was calculated as the slope of the moment-curvature diagram. The average flexural stiffness of each group is presented in Table 3. It indicates that the addition of fiber mat layers or intermediate GFRP layers increased the flexural stiffness of the specimens. In this study, the moment-curvature (MC) method complemented the method based on the displacement of two span configurations (known as ASTM method, discussed in the next section). Both MC and ASTM methods provide the flexural stiffness of sandwich system independently and the effect of shear deformation is included in both methods. It should be noted that the MC method would provide an approximation, if the core material was too flexible under shear inducing large shear deformations and violating the linear strain profile assumption of the MC method.

3.5. Flexural and Shear Stiffness Calculations (ASTM Method)

Flexural stiffness D and shear stiffness U can be calculated according to ASTM D7250 [25] using the overall stiffness K of a given specimen type at two different span lengths as follows [26]:

$$\frac{1}{K_i} = \frac{2{S_i}^3 - 3S_i{L_i}^2 + {L_i}^3}{96D} + \frac{S_i - L_i}{4U} \quad (1)$$

where S is the support span, L is the loading span, i denotes the parameters based on the short and long spans as presented in Table 1. The overall stiffness K of each group of specimens was taken from Table 2. The first term of the equation is related to the bending deflection while the second term is related to the shear deflection. The system of two equations and two unknowns based on the form presented in Equation 1 was solved based on two spans of the test specimens to obtain both flexural and shear stiffness of each type of sandwich specimens.

Table 3 shows the flexural stiffness D calculated based on this method (hereafter called ASTM method) described above as well as the flexural stiffness calculated from the slope of the moment-curvature diagrams calculated in the previous section. The table shows that the ASTM method tends to predict slightly higher flexural stiffnesses than the moment-curvature method (MC method). The ratio of the flexural stiffness obtained based on the ASTM method to that of the moment-curvature method was calculated for each group of the specimens. The average ratio is 1.11, which indicates a good agreement between the two methods. The average flexural stiffness obtained from the two methods is also presented in Table 3 to be used later verifying an analytical method.

The shear stiffness U of each group of specimens was also obtained from Equation 1 and presented in Table 3. Based on the results, the shear modulus G of core can then be calculated as follows:

$$G = U\frac{h-2t}{(h-t)^2 b} \quad (2)$$

where h is the thickness of the sandwich beam, t is the thickness of facesheet, and b is the width of the beam. The dimensions of h and b used in Equation 2 are based on the averages from the three identical specimens tested of each core configuration. The results indicate that the shear modulus G of the core made of 1, 2, and 3 layers of the fiber mat layer is 144, 134, and 130 MPa, respectively. The higher shear modulus of the core made of one layer of fiber mat might be related to its smaller thickness and absorbing more resin from the facesheets in comparison with the core made of two and three layers of fiber mat. The average shear modulus of 136 MPa will be used for the analytical study presented in the next section. It should be highlighted that the sandwich flexure test provides an approximate shear property for the core. More research using a direct shear test method is recommended in the future.

4. ANALYTICAL STUDY

An analytical study is presented in this section to predict the overall stiffness and load capacity of the layered sandwich specimens tested in the experimental study. After verification against the test data, a parametric study is performed on parameters which were not considered in the experimental study.

4.1. Flexural Stiffness

The flexural stiffness D can be determined for each specimen using calculations tailored for each specimen type using Equations 3, 4, and 5. The calculations assume that any layers with a sandwich specimen are perfectly bonded together. The cross-section of each specimen has a width b and total thickness h. The GFRP layer has a thickness t and the individual fiber mat core layer has a thickness c. The flexural stiffness D of a cross-section without any intermediate

GFRP layers is the sum of the flexural stiffness of its core and facesheet layers, calculated about its centroidal axis as follows:

$$D = E_f \frac{bt^3}{6} + E_f \frac{btd^2}{2} + E_c \frac{b(n_c c)^3}{12} \quad (3)$$

where E_f and E_c are the modulus of elasticity of the facesheet and core, respectively, d is the distance between the centerlines of the top and bottom GFRP facesheets, n_c is the number of fiber mat core layers, and t is the thickness of the facesheet. It should be mentioned that the nominal thickness of 1.3 mm per layer of GFRP was used, which is tied to the modulus of elasticity of the facesheet reported as 27.4 GPa by the manufacturer of the fiberglass fabric and resin. It should be noted that the potential variation in thicknesses of GFRP could have a drastic impact on the results if the modulus of elasticity of GFRP was not tied to the thickness. Equation 3 is applicable for the F1, F2, and F3 specimens with taking n as 1, 2, and 3, respectively. Similar equations were also developed to calculate the flexural stiffness D of the specimens with intermediate GFRP layer (i.e., F2-G and F3-G). For the F2-G specimens that include one intermediate GFRP layer and two fiber mat core layers, the flexural stiffness is calculated as:

$$D = E_f \left(\frac{bt^3}{4} + \frac{btd^2}{2} \right) + E_c \left(bc^3 + \frac{bc(c+t)^2}{2} \right) \quad (4)$$

For the F3-G specimens that include two intermediate GFRP layers and three fiber mat core layers, the flexural stiffness is calculated as:

$$D = E_f \left(\frac{bt^3}{3} + \frac{5btd^2}{9} \right) + E_c \left(\frac{bc^3}{4} + 2bc(c+t)^2 \right) \quad (5)$$

The flexural stiffness of each specimen was calculated using the average of the dimensions for the three identical specimens tested of each sandwich type and is shown with the flexural stiffnesses calculated based on the test methods in Table 3. The ratio of the flexural

stiffnesses obtained from the test method over that of obtained from the analytical method (model) is also presented in Table 3. The test/model ratio ranges from 0.93 to 1.00 with an average of 0.95 indicating the analytical method predicts the flexural stiffness D slightly lower that the experimental values. Overall, there is a very good agreement between the model and test data.

4.2. Bending and Shear Stiffness

The overall stiffnesses K of each specimen type were also calculated through the corresponding shear deflection Δ_s and bending deflection Δ_b under the application of the load P under four-point bending as follows:

$$K = \frac{P}{\Delta_s + \Delta_b} \tag{6}$$

$$\Delta_s = \frac{P(S-L)}{4U} \tag{7}$$

$$\Delta_b = \frac{P(2S^3 - 3SL^2 + L^3)}{96D} \tag{8}$$

The flexural stiffness D was calculated using Equations 3 to 5. The shear stiffness U was calculated using Equation 2 and the shear modulus G was taken 136 MPa per Table 3. The elastic modulus E_c of the core was found 396 MPa using $E_c=2G(1+\nu)$, where the Poisson's ratio ν was assumed 0.3. Poisson's ratio of the core needs to be verified from tension tests of the core in the future. It should be highlighted that the elastic modulus of the core is much less than that of the GFRP facesheets (i.e. 27.4 GPa) and the assumption of Poisson's ratio does not affect the flexural stiffness of the sandwich cross-section and the overall stiffness calculations.

The overall stiffness K calculated for specimens with span of 300 mm is shown in Figure 8(a) along with the overall experimental stiffness averaged from the slopes of the load-deflection diagrams of each specimen tested for a given sandwich type. The error bars show a standard

deviation above and below the average values. Overall, the figure shows that the analytical values are very close to the experimental values indication the goodness of the analytical method.

Based on Equations 7 and 8, the contribution of bending and shear into overall analytical stiffness of the specimens was calculated and presented in Figure 8(b). The figure indicates that shear has only a limited contribution ranging from 3% for F1 specimens to 22% for F3-G specimens. The shear contribution increases as the number of fiber mat core layers increases. Overall, the results show that the fiber mat core used in this study is stiff enough in shear to accommodate the composite action between the GFRP facesheets.

4.3. Peak Load

Two failure modes are most probable among the specimens within this study: namely top facesheet crushing (TFC) and core shear (CS). The failure load P_{TFC} at which top facesheet crushing occurs can be determined using the equation developed by Triantafillou and Gibson [27]:

$$P_{TFC} = \frac{2\sigma_{fc} btd}{S - L} \tag{9}$$

where σ_{fc} is the compressive strength of the facesheet material, in this case the unidirectional GFRP. The compressive strength of the facesheet material was assumed to be 80% that of the tensile strength of the facesheet material as shown by Khorramian and Sadeghian [28]. The failure load P_{CS} at which core shear occurs can be determined using the equation below derived from basic mechanics and the treatment of a sandwich cross-section as an I-beam:

$$P_{CS} = \frac{8\tau_c I}{nh^2 - nc^2 + c^2} \tag{10}$$

where τ_c is the shear strength of the core material taken as 3.55 MPa per the manufacturer, n is the ratio of the modulus of elasticity of the facesheet material to that of the core material, and I is the moment of inertia of the cross-section transformed with the width of the core being divided by the ratio of the moduli of elasticity. The peak load of each specimen tested in this study was predicted and is shown in Figure 9 along with the average peak loads from the tests. The figure shows that the peak loads were predicted accurately.

The analytical model presented in this section was implemented to plot the load-deflection, load-strain, and moment-curvature diagrams of the test specimens based on the peak load and corresponding displacement, strain, and curvature of the test specimens at mid-span, respectively. The results are shown in Figures 5, 6, and 7 using dotted lines along with experimental diagrams. Overall, the figure show that the analytical model can successfully predict the behaviour of the test specimens.

4.4. Parametric Study

A parametric study was performed using the analytical model for the prediction of failure load and deflection of cases not considered in the experimental study presented above. The aim of the parametric study is to gain insight into the effect of GFRP facesheet thickness, fiber mat core thickness, and the inclusion of intermediate GFRP layers within the core on load-deflection behaviour. The average core shear modulus found from the test results and its corresponding core modulus of elasticity was used for the analytical modeling for the parametric study. It should be noted that the current study only includes the two observed failure modes (i.e. top facesheet crushing and core shear failure). Although this may capture the general load-deflection behavior, it is important to note that it may not capture the failure load accurately as the failure mechanism may change (e.g. thinner facesheet may lead to premature outward wrinkling).

4.3.1. Effect of GFRP Facesheet Thickness

Figure 10 shows the load-deflection diagrams created using the model for one, two, and three-layer fiber mat core sandwich beams with a span of 300 mm with varying thicknesses of facesheet layers, where SX indicating the number of GFRP layers on the outer faces with X indicating one, two, or three GFRP layers. The diagram indicates that additional GFRP facesheets added to the outer face enhance the overall stiffness of the sandwich beam. The change from one to two GFRP outer facesheet layers leads to an appreciable increase in the overall stiffness followed by a smaller increase when changing from two to three GFRP outer facesheet layers.

4.3.2. Effect of Fiber Mat Core Thickness

The load-deflection diagrams created using the model for varying fiber mat core thickness is shown in Figure 11 with models being created for cases of sandwich beams with one, two, three, and four fiber mat core layers with two or three layers of GFRP facesheet. Additional fiber mat core layers increase the strength and overall stiffness of a sandwich beam made from the synthetic fiber mat core and unidirectional fiberglass fabric used in this study. The use of three outer GFRP facesheets instead of two leads to a small increase in the strength of a sandwich beam and an increase in the overall stiffness of the sandwich beam as discussed previously.

4.3.3. Effect of GFRP Layer in Core

Figure 12 shows the load-deflection diagrams created using the model for sandwich beams containing two, three, and four fiber mat core layers with varying thicknesses of intermediate GFRP layers between the fiber mat cores, where GY indicates the number of GFRP layers between fiber mat layers, being either zero, one, or two layers of GFRP facesheets. Each case in Figure 12 was considered with two outer GFRP facesheet layers. The load-deflection behaviour

indicates that the addition of intermediate GFRP layers between fiber mat cores increase both the strength and overall stiffness of a sandwich beam. The modeled behaviour also indicates that the use of two intermediate GFRP facesheets between fiber mat layers instead of only one GFRP layer could increase the strength and overall stiffness of the sandwich beam. The models could be improved given accurate information of the compressive strength of the GFRP face material. Testing large- scale specimens are also recommended for the future studies.

5. CONCLUSIONS

In this study, a total of 30 small-scale sandwich beams were fabricated with GFRP facesheets and a thin, non-woven continuous strand polyester fiber mat core. Specimens were fabricated with one, two, and three layers of fiber mat cores and with the inclusion of intermediate GFRP facesheets between fiber mat layers at span lengths of 200 mm, 300 mm, and 400 mm and tested under four-point bending. The load-deflection, load-strain, and moment-curvature behaviour were analyzed. Based on the results, values for core shear modulus, shear stiffness, and flexural stiffness were calculated. An analytical model was successfully developed and presented to predict both failure load, shear and flexural stiffness, and deflection of varying core layouts. This analytical model was used for a parametric study on cases not considered during the experimental study to investigate the behaviour given certain core layouts. The experimental results and load-deflection diagrams generated by the analytical model indicate that additional outer GFRP facesheets can increase the overall stiffness of sandwich beams and additional fiber mat core layers can increase both the strength and the overall stiffness of sandwich beams. The addition of intermediate layers is shown to increase both the strength and overall stiffness of sandwich beams. The results indicate that the GFRP facesheet and fiber mat core used in this

study are promising options for use in structural applications, including use in non-conventional applications where a curved shape would be necessary. The fiber mat core materials flexibility would allow for use in curved shapes and the models indicates that the sandwich structures fabricated using this material undergo minimal shear deflection, with the majority of its deflection being due to bending. The new generation of thin fiber mat cores can provide a breakthrough solution for the challenges of the conventional fiber mat cores opening new avenues for curved-shape applications. However, more studies are required to better understand the material's behaviour in large-scale sandwich structures and curved applications.

6. ACKNOWLEDGEMENTS

The authors of this paper would like to acknowledge the efforts of the technicians at Dalhousie University's Civil and Resource Engineering Department, Jesse Keane, Jordan Maerz, and Brian Kennedy, who helped immensely with the setup, instrumentation and testing process. In addition, the authors acknowledge the National Science and Engineering Research Council of Canada (NSERC) for the Undergraduate Student Research Award (USRA) for the first author and QuakeWrap Inc. (Tucson, AZ, USA) for providing the fiberglass and fiber mat core as well as the epoxy resin used in specimen fabrication. The authors would also like to acknowledge the efforts of undergraduate student, Yuchen Fu for his assistance with fabrication and testing, and PhD student Dillon Betts for his guidance and technical support.

7. REFERENCES

[1] Allen, H. G. (1969). *Analysis and Design of Structural Sandwich Panels*. Pergamon Press Ltd, Oxford, United Kingdom.

[2] Manalo, A., Aravinthan, T., and Benmokrane, B. (2017). State-of-the-art review on FRP sandwich systems for lightweight civil infrastructure. *Journal of Composites for Construction*, 21(1), 1-16.

[3] Wang, L., Liu, W., Fang, H., and Wan, L. (2015). Behavior of sandwich wall panels with GFRP face sheets and a fiber mat-GFRP web core loaded under four-point bending. *Journal of Composite Materials,* 49(22), 2765-2778.

[4] Mathieson, H., and Fam, A. (2015). In-plane bending and failure mechanism of sandwich beams with GFRP skins and soft polyurethane fiber mat core. *Journal of Composites for Construction*, 20(1), 1-10.

[5] Zenkert, D., and Burman, M. (2011). Failure mode shifts during constant amplitude fatigue loading of GFRP/fiber mat core sandwich beams. *International Journal of Fatigue,* 33(2), 217-222.

[6] CoDyre, L., Mak, K., and Fam, A. (2018). Flexural and axial behaviour of sandwich panels with bio-based flax fibre-reinforced polymer skins and various fiber mat-core densities. *Journal of Sandwich Structures and Materials,* 20(5), 595-616.

[7] Sadeghian, P., Hristozov, D., and Wroblewski, L. (2016). Experimental and analytical behaviour of sandwich composite beams: Comparison of natural and synthetic materials. *Journal of Sandwich Structures and Materials,* 20(3), 287-307.

[8] Betts, D., Sadeghian, P., and Fam, A. (2018). Experimental behavior and design-oriented analysis of sandwich beams with bio-based composite facings and fiber mat cores. *Journal of Composites for Construction*, 22(4), 1-12.

[9] Zenkert, D. (1997). *The Handbook of Sandwich Construction.* Engineering Materials Advisory Services Ltd, Cradley Heath, West Midlands, United Kingdom:

[10] Atas, C., and Sevim, C. (2010). On the impact response of sandwich composites with cores of balsa wood and PVC fiber mat. *Composite Structures,* 93(1), 40-48.

[11] Lingaiah, K., and Suryanarayana, B. G. (1991). Strength and stiffness of sandwich beams in bending. *Experimental Mechanics,* 31(1), 1-7.

[12] Belouettar, S., Abbadi, A., Azari, Z., Belouettar, R., and Freres, P. (2009). Experimental investigation of static and fatigue behaviour of composites honeycomb materials using four point bending tests. *Composite Structures,* 87(3), 265-273.

[13] Ferdous, W., Manalo, A., Aravinthan, T., and Fam, A. (2018). Flexural and shear behaviour of layered sandwich beams. *Construction and Building Materials,* 173, 429-442.

[14] Osei-Antwi, M. De Castro, J., Vassilopoulos, A., and Keller, T. (2014). Modeling of axial and shear stresses in multilayer sandwich beams with stiff core layers. *Composite Structures,* 116(1), 453-460.

[15] McCracken, A. and Sadeghian P. (2018). Partial-composite behavior of sandwich beams composed of fibreglass facesheets and woven fabric core. *Thin-Walled Structures,* 131, 805-815.

[16] Salleh, Z., Islam, M. M., Epaarachchi, J. A., and Su, H. (2016). Mechanical properties of sandwich composite made of syntactic fiber mat core and GFRP skins. *AIMS Materials Science,* 3(4), 1704-1727.

[17] Gupta, N., Woldesenbet, E., Hore, K., and Sankaran, S. (2002). Response of syntactic fiber mat core sandwich structured composites to three-point bending. *Journal of Sandwich Structures & Materials,* 4(3), 249-272.

[18] Mines, R. A. W., Worrall, C. M., & Gibson, A. G. (1994). The static and impact behaviour of polymer composite sandwich beams. *Composites,* 25(2), 95-110.

[19] Mines, R. A. W., and Jones, N. (1995). Approximate elastic-plastic analysis of the static and impact behaviour of polymer composite sandwich beams. *Composites*, 26(12), 803-814.

[20] Kolat, K., Neşer, G., and Özes, Ç. (2007). The effect of sea water exposure on the interfacial fracture of some sandwich systems in marine use. *Composite Structures*, 78(1), 11-17.

[21] Aquino, E. M. F., Sarmento, L. P. S., Oliveira, W., and Silva, R. V. (2007). Moisture effect on degradation of jute/glass hybrid composites. *Journal of Reinforced Plastics and Composites*, 26(2), 219-233.

[22] Russo, A., and Zuccarello, B. (2007). Experimental and numerical evaluation of the mechanical behaviour of GFRP sandwich panels. *Composite Structures*, 81(4), 575-586.

[23] Ude, A. U., Ariffin, A. K., and Azhari, C. H. (2013). Impact damage characteristics in reinforced woven natural silk/epoxy composite face-sheet and sandwich fiber mat, coremat and honeycomb materials. *International Journal of Impact Engineering*, 58, 31-38.

[24] ASTM D7249 (2018). *Standard Test Method for Facing Properties of Sandwich Constructions by Long-Beam Flexure*. American Society for Testing and Materials, West Conshohocken, PA, USA.

[25] ASTM D7250 (2016). *Standard Practice for Determining Sandwich Beam Flexural and Shear Stiffness*. American Society for Testing and Materials, West Conshohocken, PA, USA.

[26] McCracken, A. and Sadeghian, P. (2018). Corrugated cardboard core sandwich beams with bio-based flax fibre. *Journal of Building Engineering*, 20, 114-122.

[27] Triantafillou, T. C., and Gibson, L. J. (1987). Failure mode maps for fiber mat core sandwich beams. *Materials Science and Engineering*, 95, 37-53.

[28] Khorramian, K., and Sadeghian, P. (2019). Material characterization of GFRP bars in compression using a new test method. Journal of Testing and Evaluation, Vol. 49, Published ahead of print, 20 May 2019, DOI: 10.1520/JTE20180873.

Table 1: Test matrix.

Case #	Specimen Group ID	Number of Core Layers	Intermediate GFRP Layer	Spans, S (mm)	Number of Specimens
1	F1-S200	1	No	200	3
2	F1-S300	1	No	300	3
3	F2-S200	2	No	300	3
4	F2-S400	2	No	400	3
5	F2-G-S300	2	Yes	300	3
6	F2-G-S400	2	Yes	400	3
7	F3-S300	3	No	300	3
8	F3-S400	3	No	400	3
9	F3-G-S300	3	Yes	300	3
10	F3-G-S400	3	Yes	400	3
Total	-	-	-	-	30

Note: One layer of GFRP was used per each facesheet.

Table 2: Summary of test results.

Case #	Specimen Group ID	Peak Load (kN)		Overall Stiffness (kN/m)		Failure Mode
		AVG	SD	AVG	SD	
1	F1-S200	2.39	0.32	186.27	13.38	TFC → TFD/CS
2	F1-S300	2.29	0.08	57.20	1.87	TFC
3	F2-S300	3.27	0.34	155.80	5.16	TFC
4	F2-S400	2.66	0.38	69.20	3.22	TFC
5	F2-G-S300	4.57	0.22	204.17	10.44	CS → TFD/TFC
6	F2-G-S400	2.83	0.23	96.23	2.35	TFC → CS
7	F3-S300	5.30	0.76	323.03	10.69	TFC
8	F3-S400	3.80	0.16	147.80	8.58	TFC
9	F3-G-S300	5.75	0.78	443.90	19.17	CS/ TFC → TFD
10	F3-G-S400	4.18	0.78	206.40	3.31	TFC

Note: AVG=Average, SD=Standard Deviation, TFC=Top Facesheet Crushing, TFD=Top Facesheet Debonding, and CS=Core Shear

Table 3: Summary of D, U, and G calculations.

Sandwich Type	Flexural Stiffness D (N-m^2)						Shear Stiffness U (kN)	Shear Modulus G (MPa)
	Test: ASTM Method	Test: MC Method	Test: Average	ASTM/ MC Ratio	Model	Test/Model Ratio		
F1	34.24	33.51	33.88	1.02	36.44	0.93	59.95	144
F2	94.38	88.30	91.34	1.07	98.23	0.93	83.37	134
F2-G	144.05	124.40	134.23	1.16	134.77	1.00	52.22	-
F3	210.80	184.97	197.88	1.14	212.26	0.93	111.26	130
F3-G	302.05	259.26	280.65	1.17	288.07	0.97	128.58	-
Average	-	-	-	1.11	-	0.95	-	136

Note: MC=moment-curvature

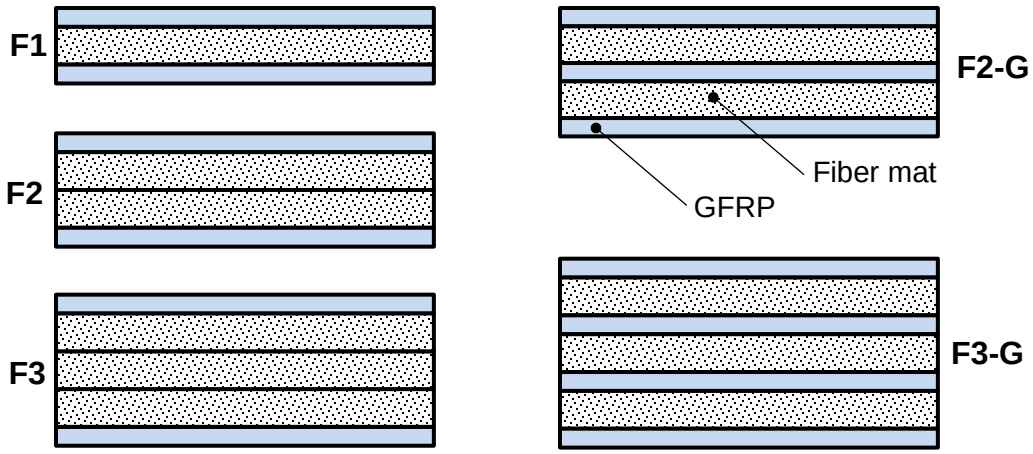

Figure 1: Specimen cross-sections (fiber mat layer thickness = 4.1 mm, GFRP layer thickness = 1.3 mm).

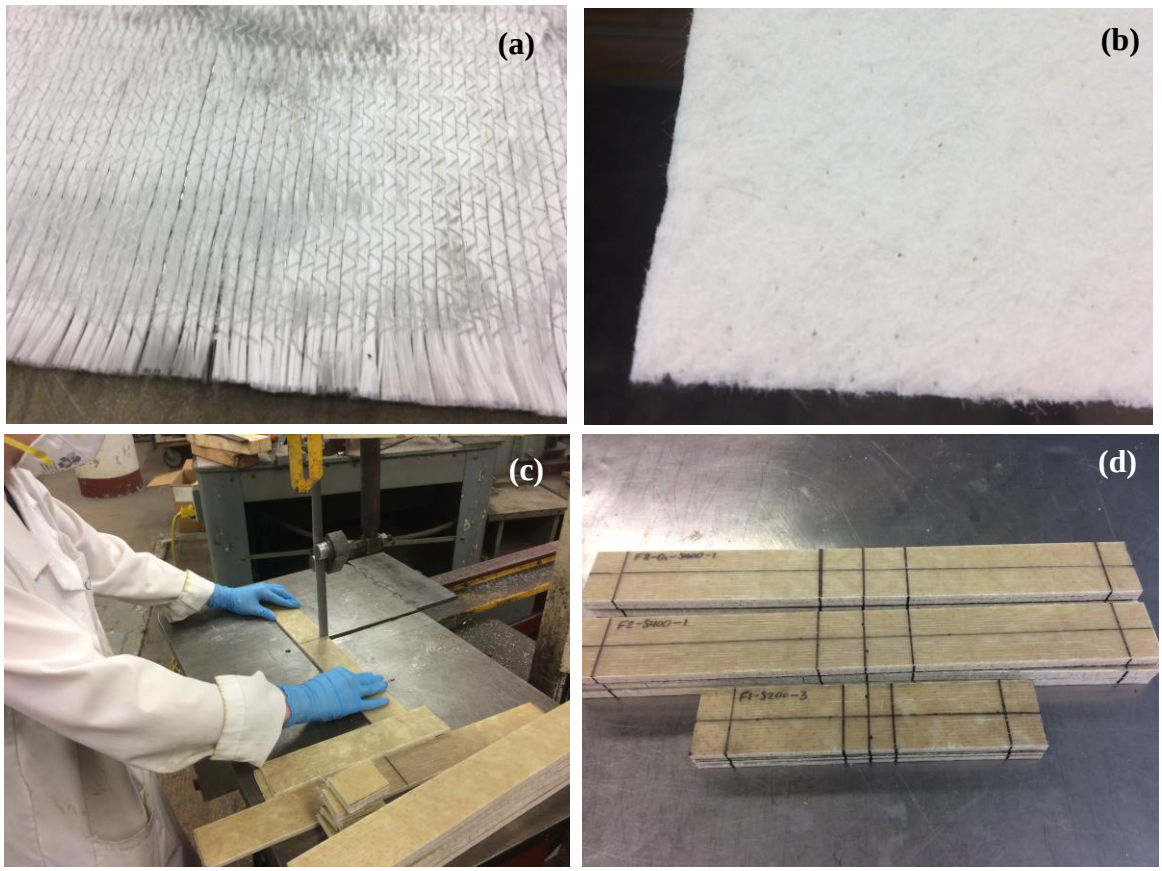

Figure 2: Specimen Fabrication: (a) dry fiberglass facing, (b) dry fiber mat core material, (c) cutting of specimens with a band saw, and (d) fabricated specimens.

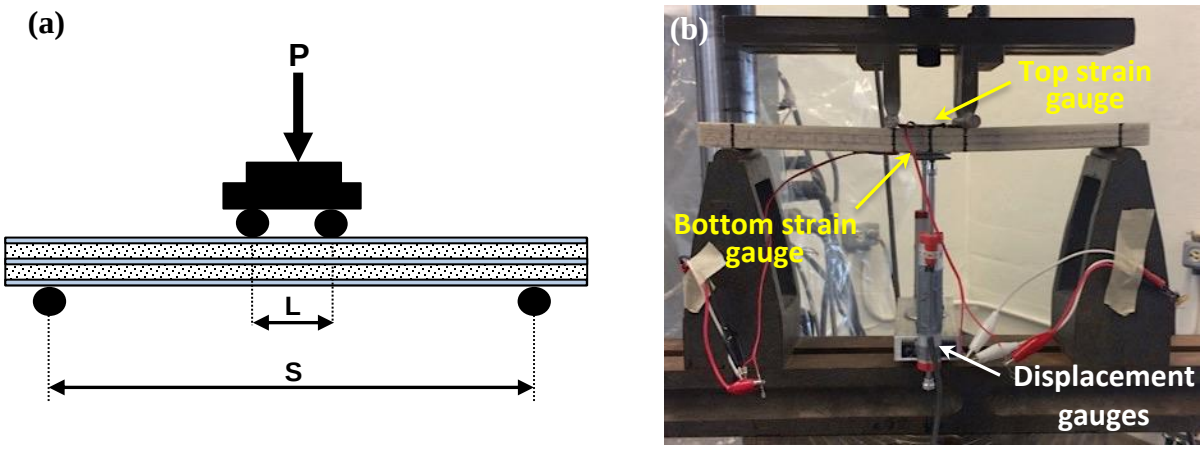

Figure 3: Test setup and instrumentation: (a) schematic and (b) photo.

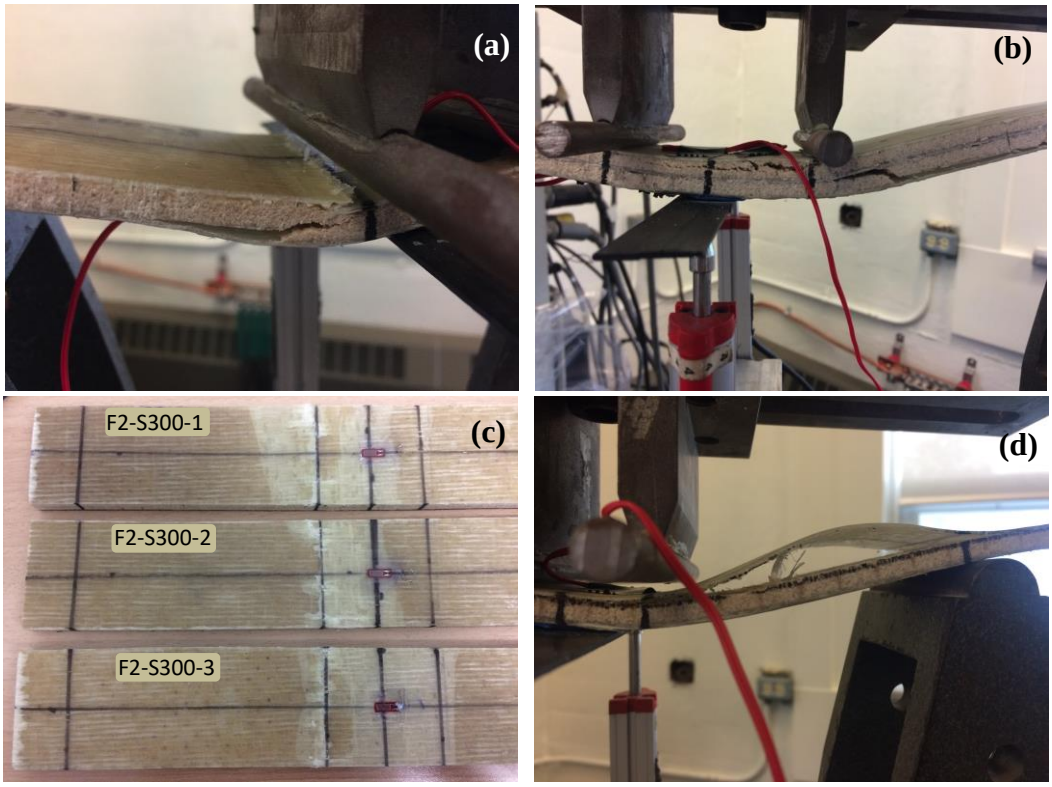

Figure 4: Failure modes: (a) core shear failure of F1-S200-3; (b) core shear failure of F2-G-S400-2; (c) top facesheet crushing failure of F2-S300; and (d) top facesheet crushing of F1-S200-2 followed with debonding and buckling.

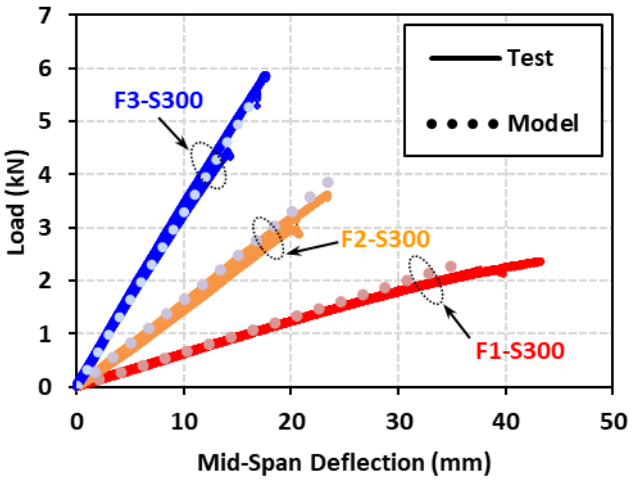

(a)

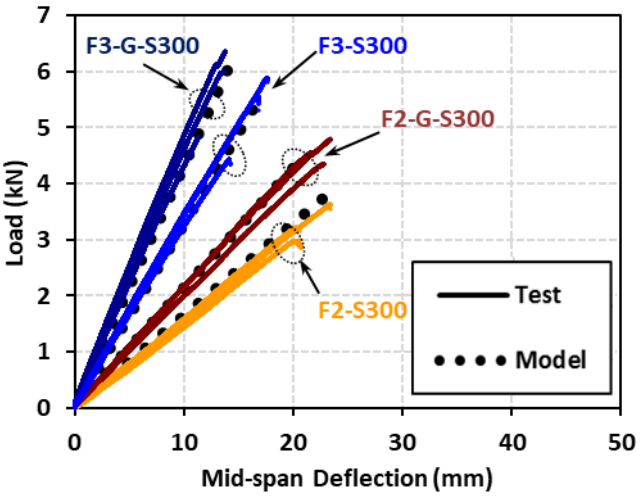

(b)

Figure 5: Load-deflection curves of specimens with span of 300 mm: (a) effect of number of core layers; (b) effect of GFRP layer between core layers.

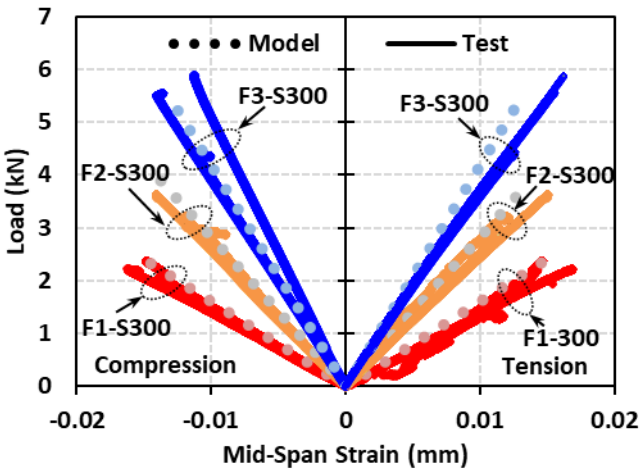

(a)

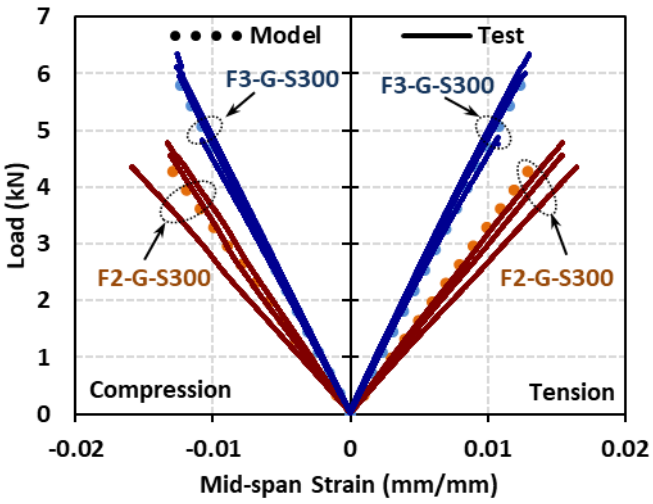

(b)

Figure 6: Load-strain curves of specimens with span of 300 mm: (a) effect of number of core layers; (b) effect of GFRP layer between core layers.

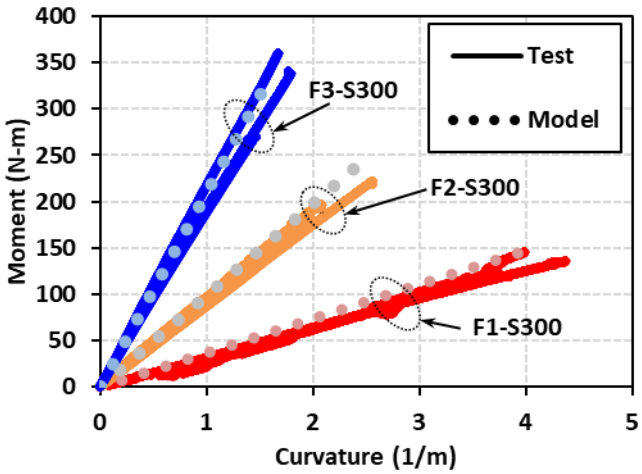

(a)

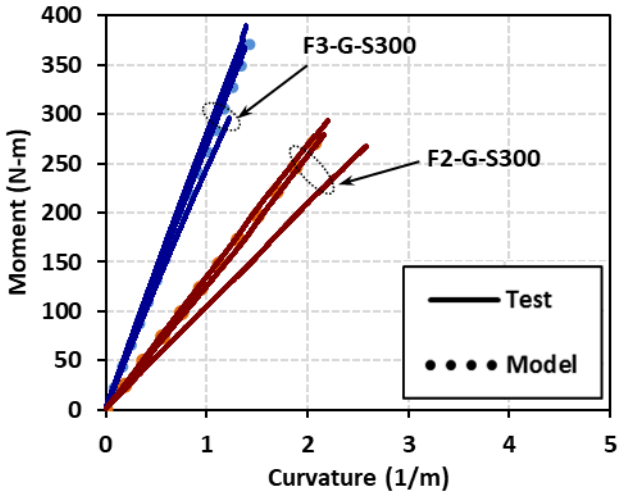

(b)

Figure 7: Moment-curvature curves of specimens with span of 300 mm: (a) effect of number of core layers; (b) effect of GFRP layer between core layers.

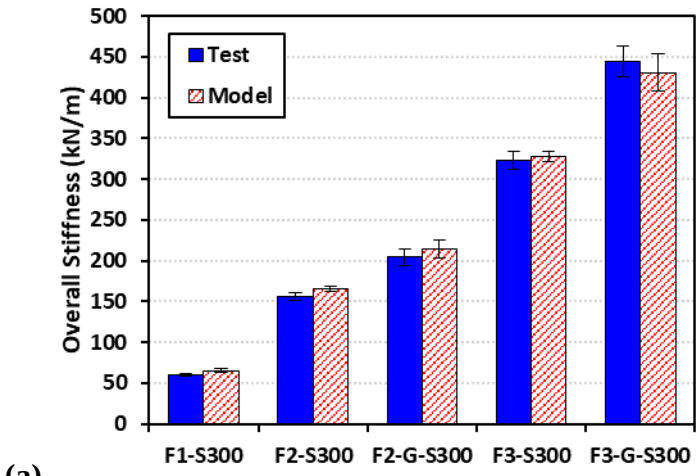

(a)

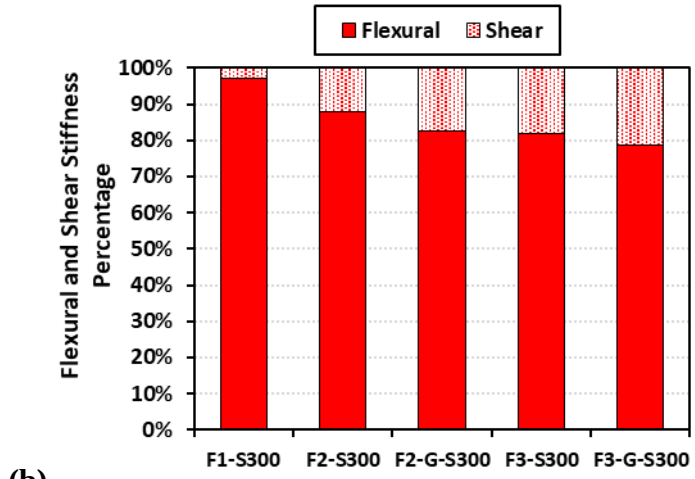

(b)

Figure 8: Stiffness comparison of specimens with span of 300 mm: (a) comparison of overall stiffness obtained from test and model; and (b) contribution flexural and shear stiffness. Note: The error bars show a standard deviation above and below the average values.

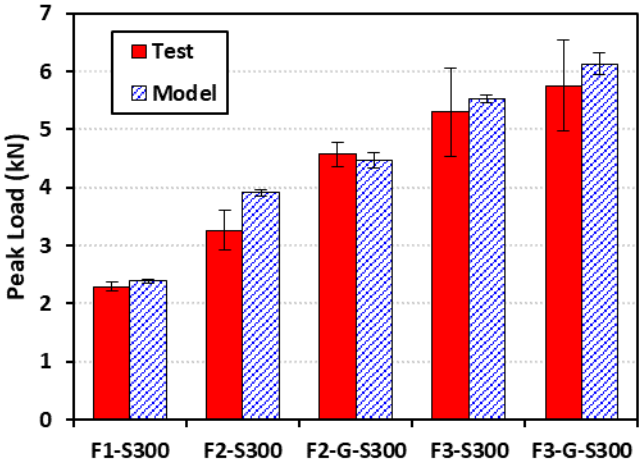

Figure 9: Comparison of experimental and analytical peak load of specimens with span of 300 mm. Note: The error bars show a standard deviation above and below the average values.

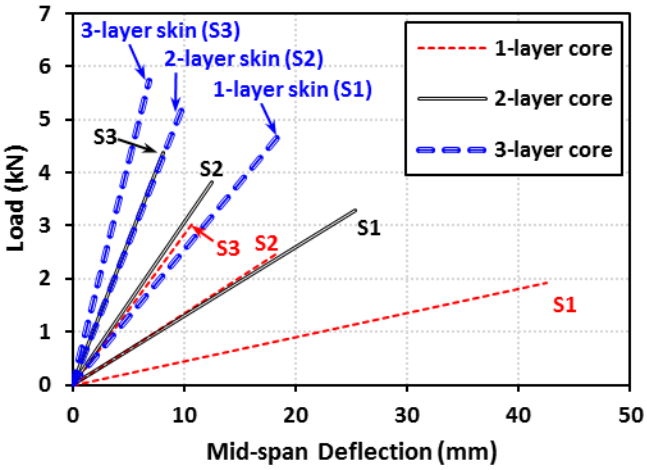

Figure 10: Effect of GFRP facesheet thickness on load-deflection behaviour

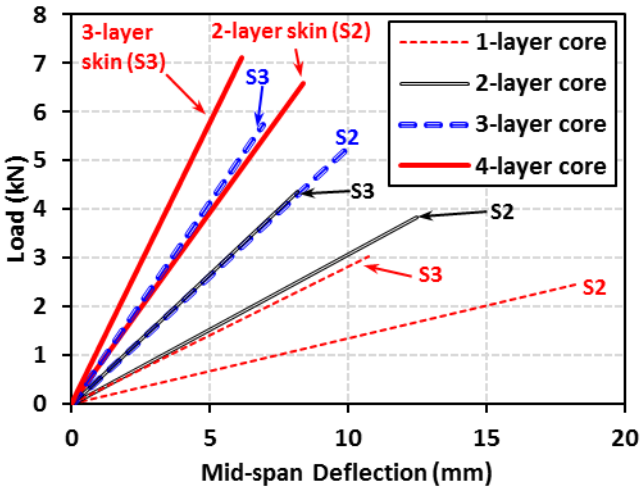

Figure 11: Effect of fiber mat core thickness on load-deflection behaviour

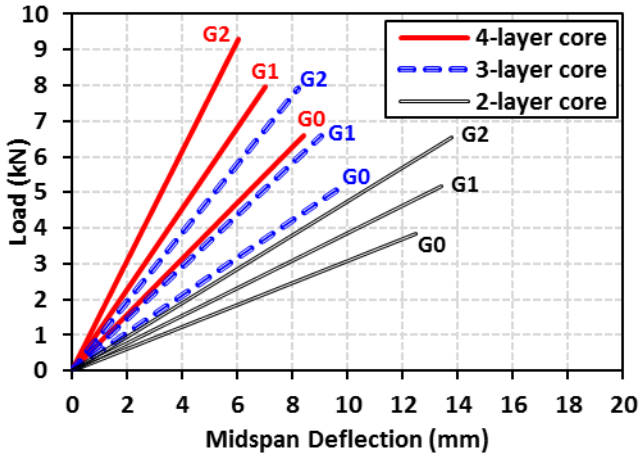

Figure 12: Effect of intermediate GFRP layers within the core (Note: all cases considered having two outer GFRP facesheet layers and G indicates the number of GFRP facesheets between fiber mat core layers)